Supporting Information for

Photocatalytic nitrogen fixation of metal-organic frameworks (MOFs) excited by ultraviolet light: Insights into the nitrogen fixation mechanism of missing metal cluster or linker defects

Wanguo Gao, Xiaoman Li*, Xu Zhang, Senda Su, Shijian Luo, Rong Huang, Yuan Jing and Min Luo*

State Key Laboratory of High-efficiency Utilization of Coal and Green Chemical Engineering, School of Chemistry and Chemical Engineering, Ningxia University, Yinchuan, Ningxia, 750021, P.R.China

*Corresponding author: Min Luo luominjy@nxu.edu.cn;

Xiaoman Li lixm2017@nxu.edu.cn

Content

The CV curves patterns of UiO-66-fresh and UiO-66-UV-vis............................**Fig. S1**

SEM and TEM images of UiO-66-UV-vis..**Fig. S2**

The photo of UiO-66-fresh and UiO-66-UV-vis...**Fig. S3**

High performance liquid chromatography (HPLC) date.....................................**Fig. S4**

Standard titration method for determination of HCO_3^- or CO_3^{2-}..........................**Fig. S5**

XRD and UV-vis DRS of UiO-66-UV-vis-ethanol and UiO-66-fresh................**Fig. S6**

UV-vis absorption spectra and Calibration curve..**Fig. S7**

Ion chromatograms date..**Fig. S8**

NH_4^+ production rate of activated UiO-66 along with the reaction time.............**Fig. S9**

UV-vis absorption spectra and Calibration curve..**Fig. S10**

N_2H_4 detection...**Fig. S11**

Comparison of the sample structure...**Fig. S12**

The CV curves patterns...**Fig. S13**

EIS of UiO-66-fresh and UiO-66-UV-vis-5th..**Fig. S14**

LSV spectra and photocurrent spectra...**Fig. S15**

N_2-TPD spectra...**Fig. S16**

N_2 adsorption-desorption isotherms and pore size distribution curves..............**Fig. S17**

The UV-vis DRS...**Fig.**

S18

XRD pattern of UiO-66-ideal..**Figure S19**

SEM and TEM images of UiO-66-ideal...**Figure S20**

Comparison of physical properties of the samples...**Table S1**

Comparison of nitrogen photofixation rate...**Table S2**

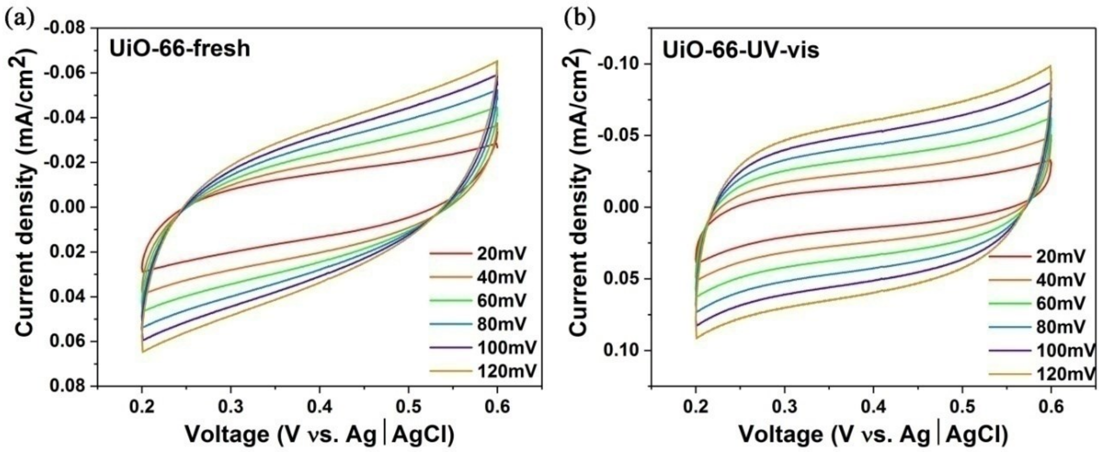

Figure S1. The cyclic voltammetry (CV) curves patterns of (a) UiO-66-fresh and (b) UiO-66-UV-vis at the scan rates range from 20 to 120 mV/s.

In the typical ECSA test, the surface area of a material is analyzed rely on electrochemical double layer capacitance (C_{dl}), which could be performed by cyclic voltammetry (CV). Therefore, the C_{dl} values were derived from CV curves using the halves of the positive current density differences at the center point of their potential ranges.

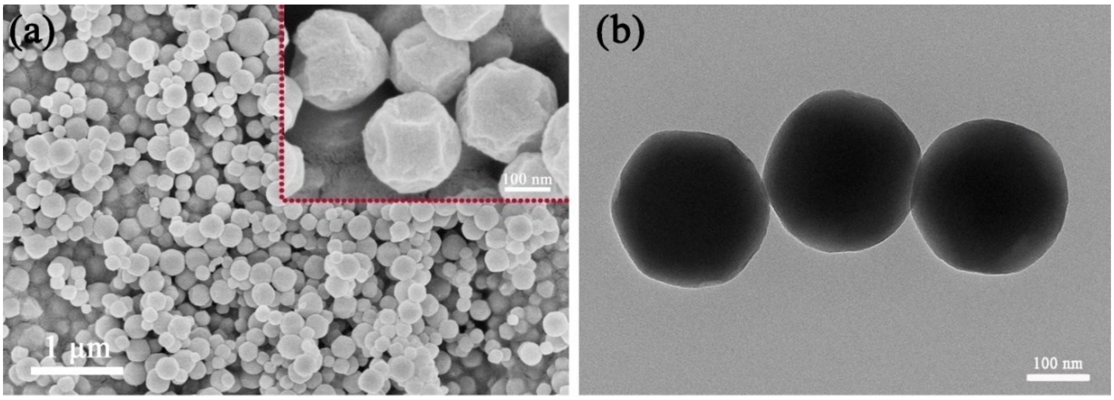

Figure S2. (a) SEM images and (b) TEM images of UiO-66-UV-vis.

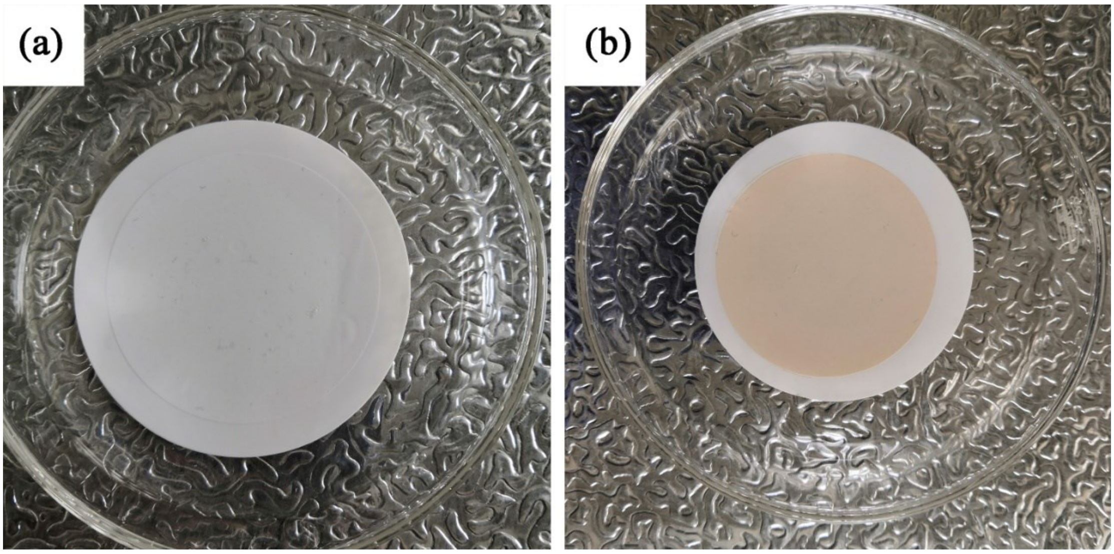

Figure S3. The photo of (a) UiO-66-fresh and (b) UiO-66-UV-vis.

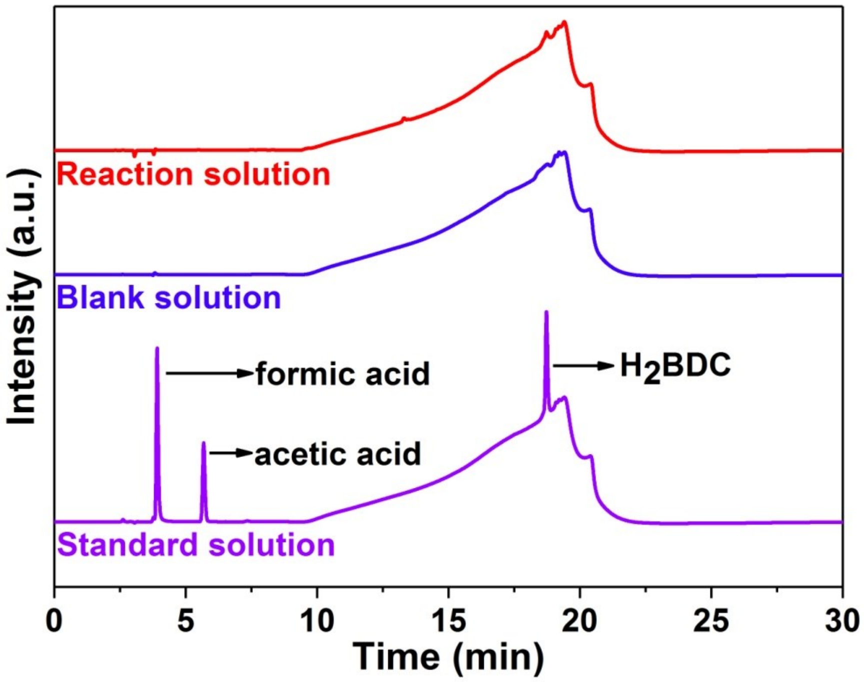

Figure S4. High performance liquid chromatography (HPLC) spectrum of the first photocatalytic solution.

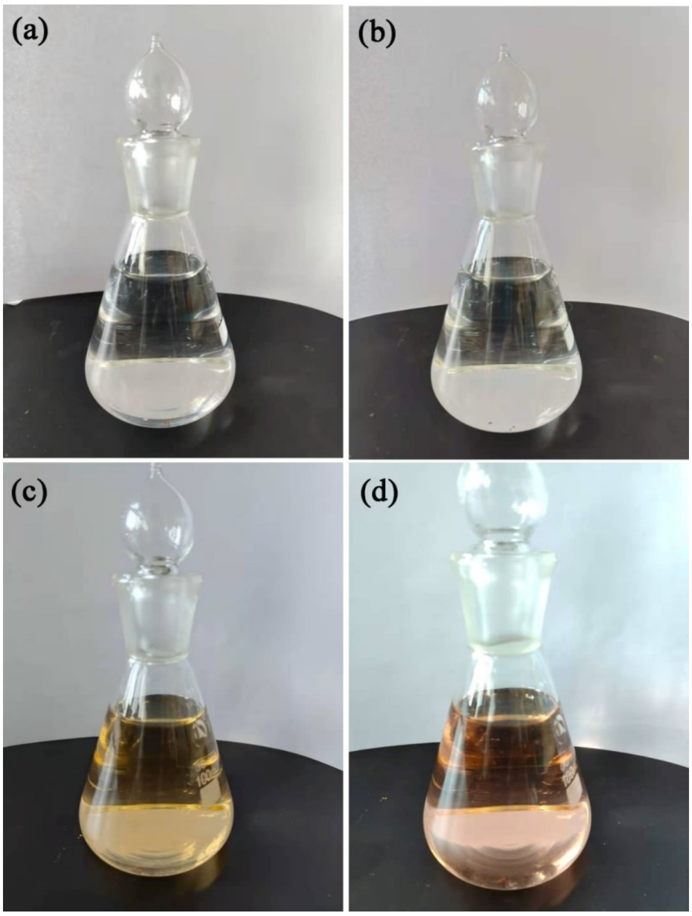

Figure S5. Standard titration method for determination of HCO_3^- or CO_3^{2-}: (a) adding phenolphthalein indicator (colorless), (b) not adding hydrochloric acid (colorless), (c) adding methyl orange indicator (orange-yellow), and (d) adding hydrochloric acid (orange-red).

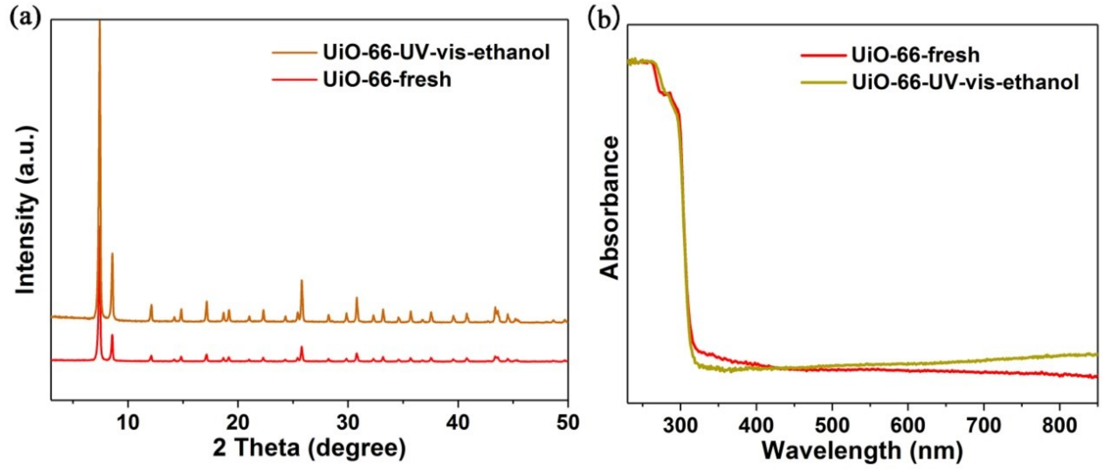

Figure S6. XRD and UV-vis DRS of UiO-66-UV-vis-ethanol and UiO-66-fresh.

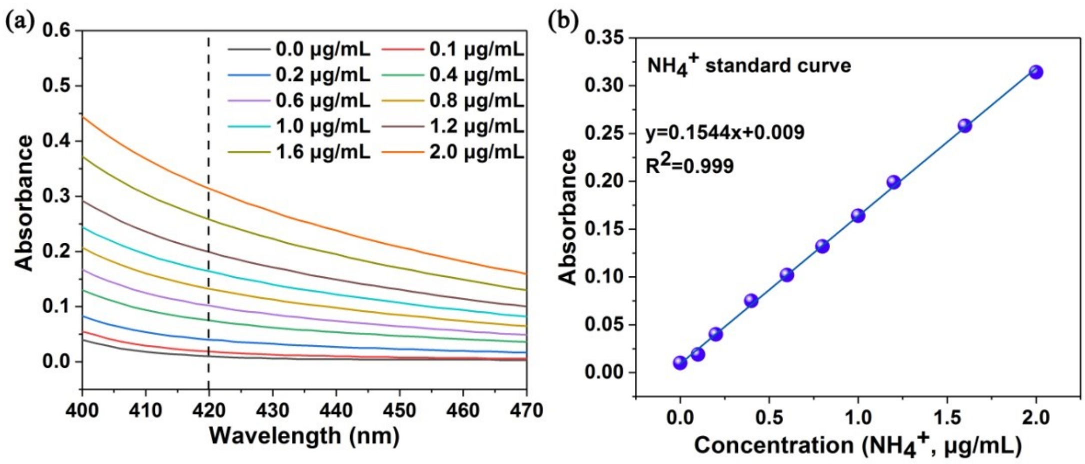

Figure S7. (a) UV-Vis absorption curves of different concentrations of NH_4^+ ions tested by Nessler's reagent method, (b) A calibration curve used to estimate the concentrations of NH_4^+ ions.

The fitting curve (y = 0.1544x + 0.009, R^2= 0.999) shows good linear relationship between the absorbance value and the NH_4^+ concentration.

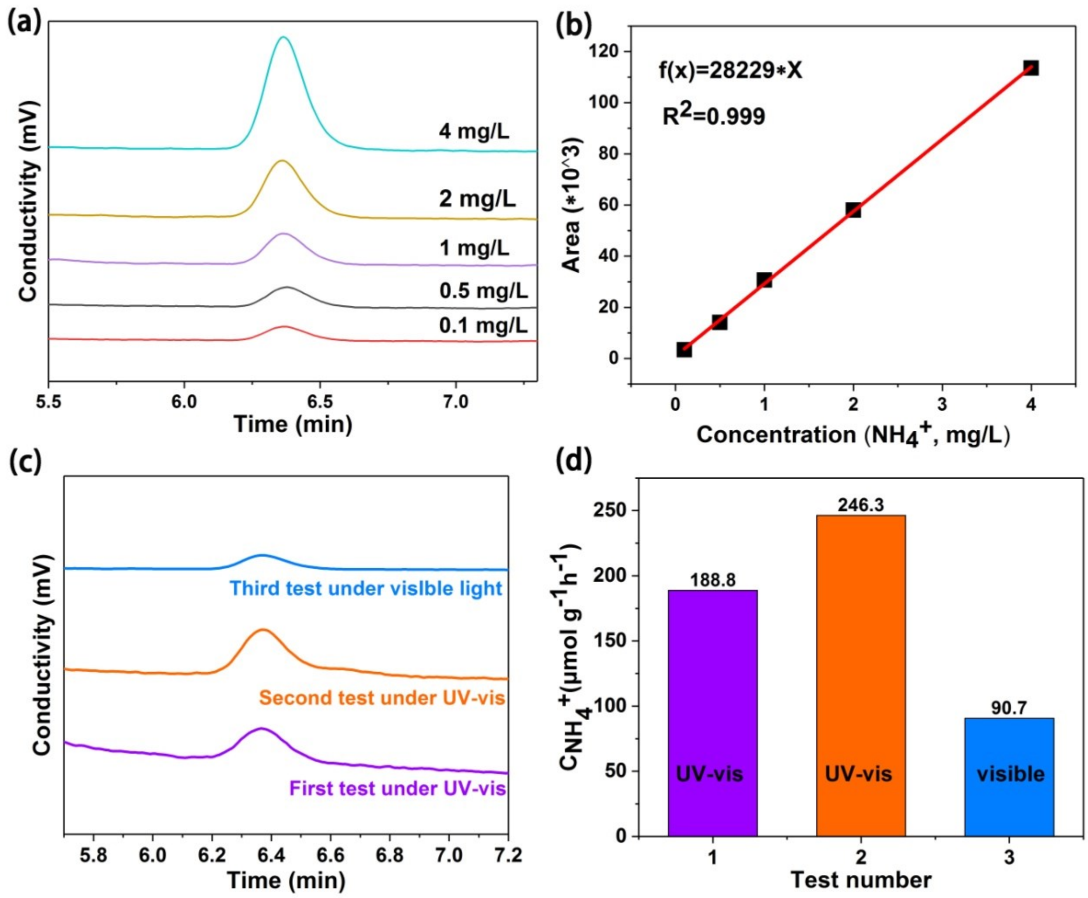

Figure S8. (a) Ion chromatograms of NH_4^+ with different concentrations in ultrapure water, (b) A calibration curve, (c) Ion chromatogram data for the solution at different light irradiation under N_2 ambient potentials, and (d) NH_3 yields calculated by ion chromatography.

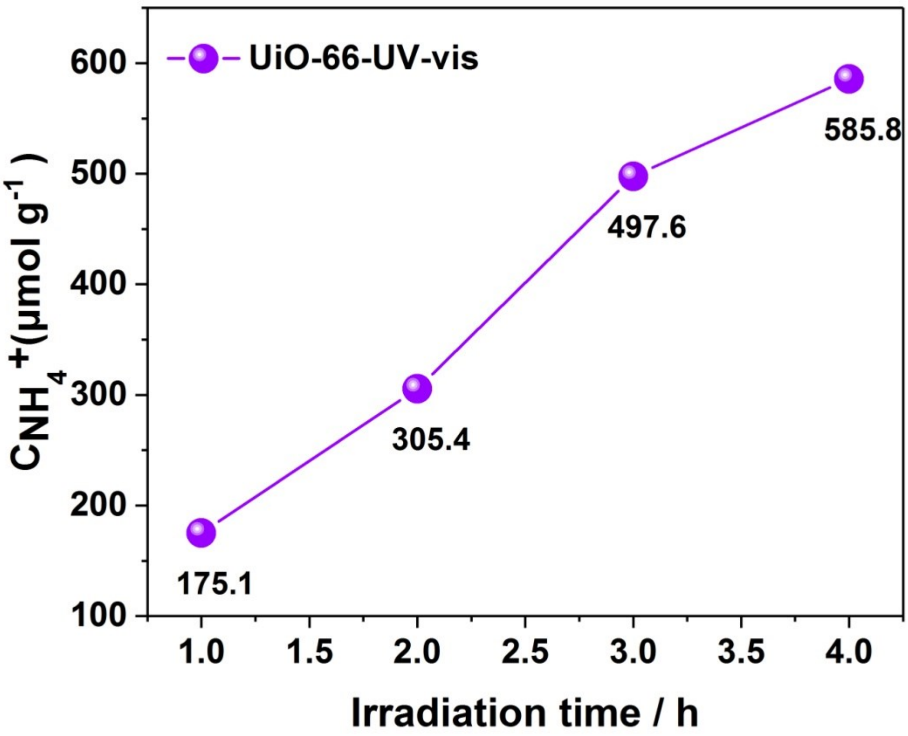

Figure S9. NH_4^+ production rate of activated UiO-66 along with the reaction time.

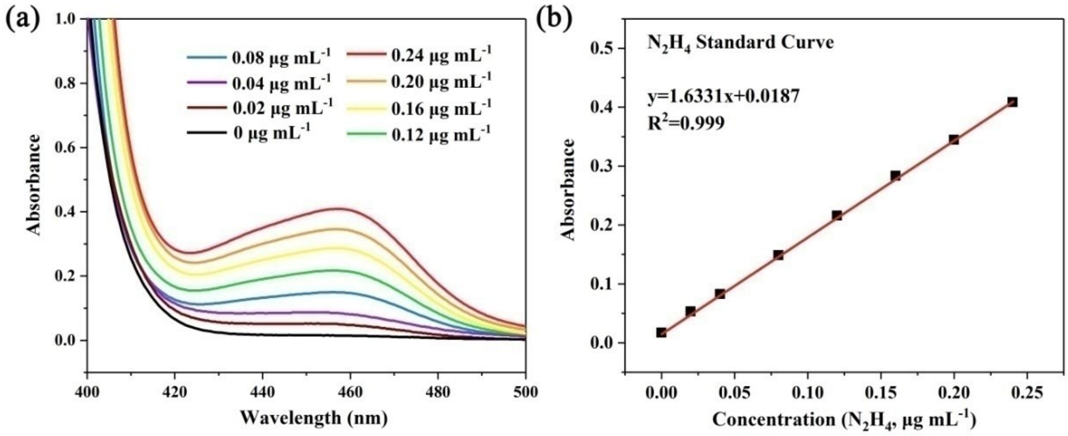

Figure S10. (a) UV-Vis absorption curves of various concentrations of N_2H_4 stained with p-$C_9H_{11}NO$ indicator, (b) A calibration curve used to estimate the concentrations of N_2H_4.

The fitting curve ($y = 1.6331x + 0.0187$, $R^2 = 0.999$) shows a good linear relation of absorbance value with N_2H_4 concentration.

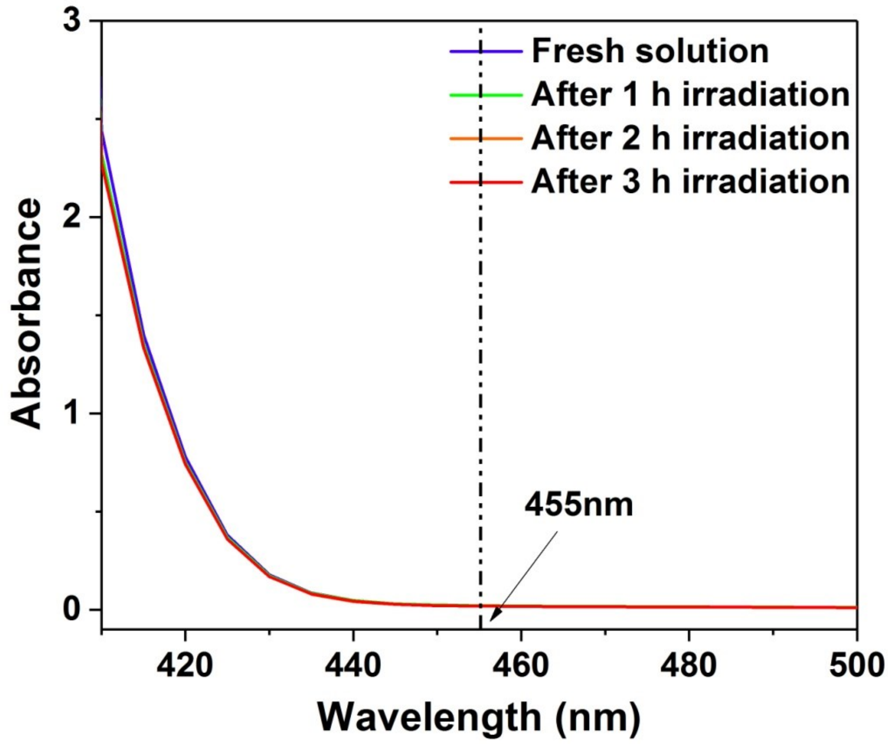

Figure S11. UV-Vis absorption spectra of the solution stained with p-$C_9H_{11}NO$ indicator after photocatalytic nitrogen fixation different time.

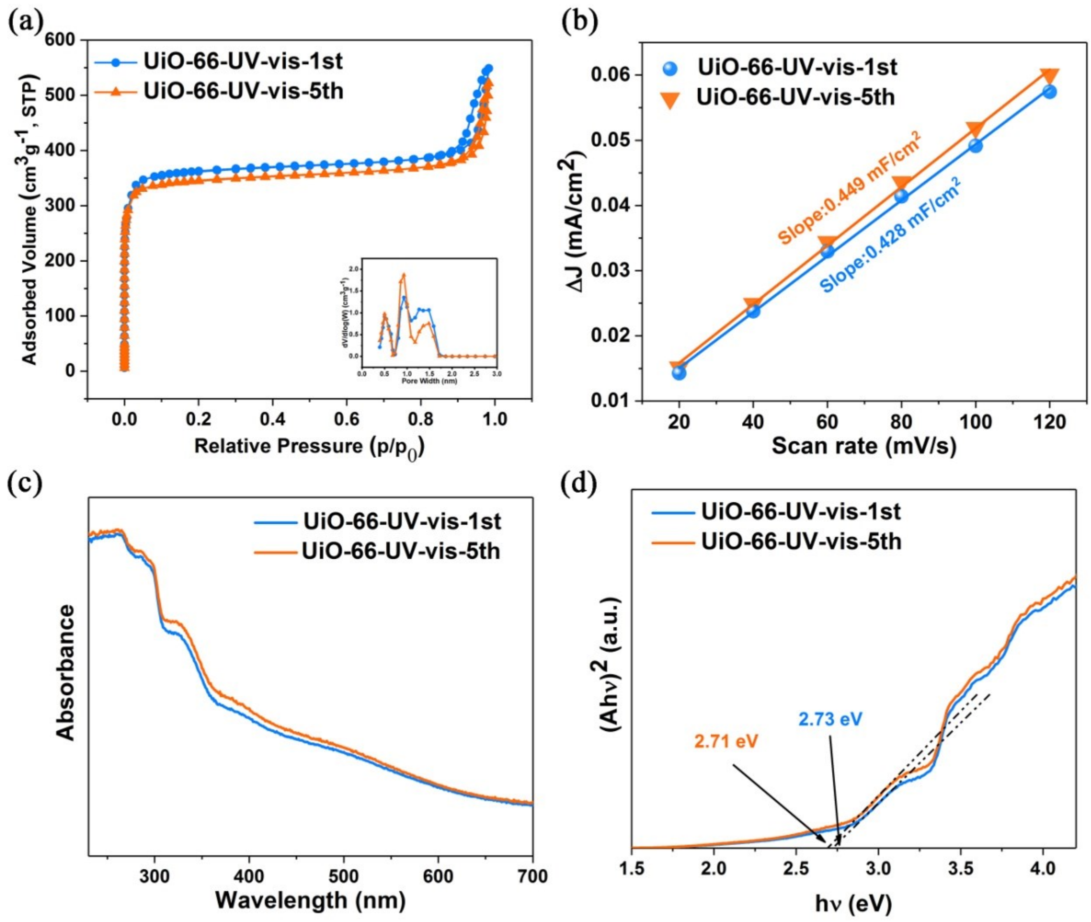

Figure S12. (a) N_2 adsorption-desorption isotherms, (b) Plot of the scan rates against the differences in the double layer charging current, (c) UV-vis DRS, and (d) Tauc plots of UiO-66-UV-vis-1st and UiO-66-UV-vis-5th.

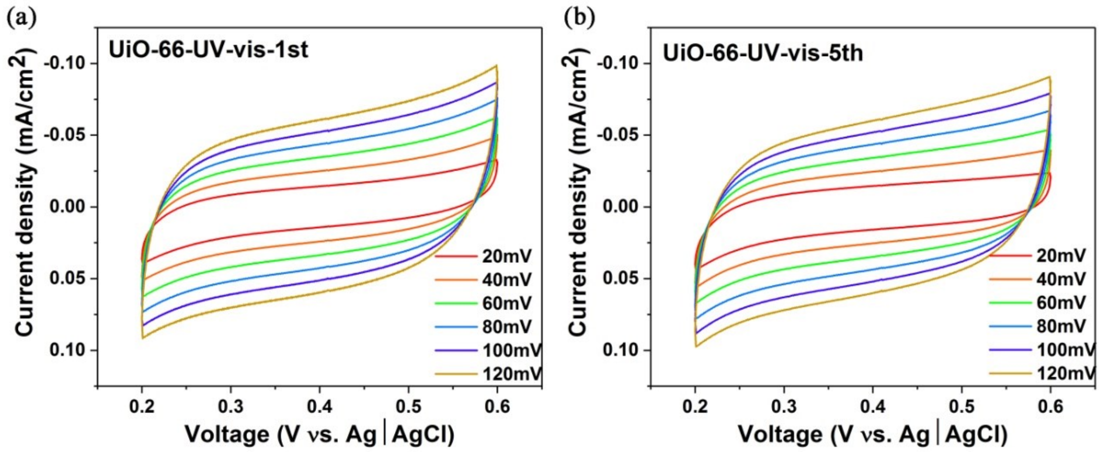

Figure S13. The cyclic voltammetry (CV) curves patterns of (a) UiO-66-UV-vis-1st and (b) UiO-66-UV-vis-5th at the scan rates range from 20 to 120 mV/s.

The calculation process is the same as Figure S1.

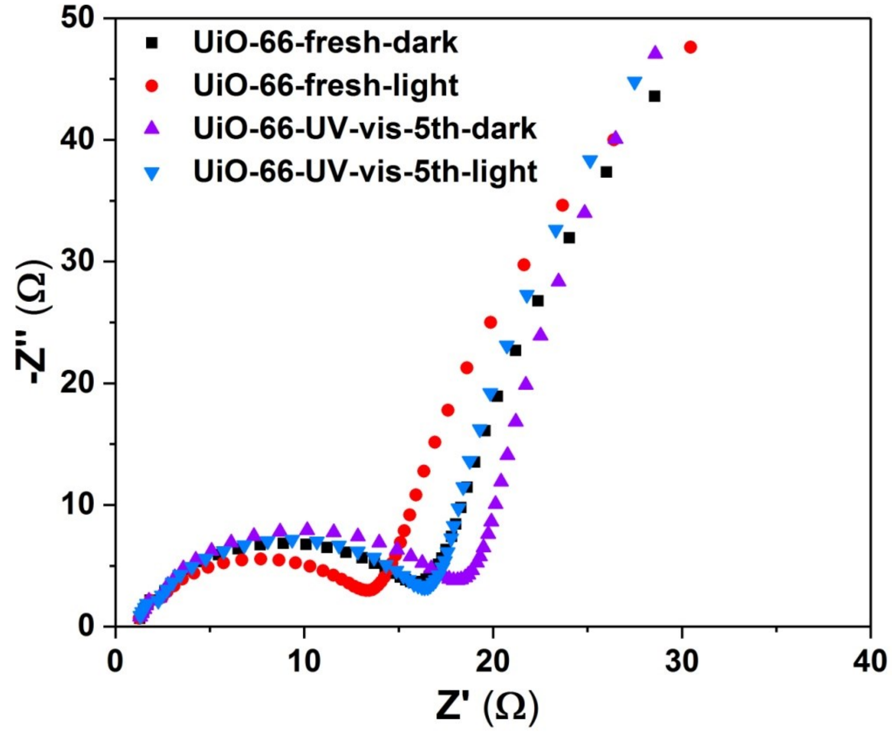

Figure S14. Electrochemical impedance spectra (EIS) of UiO-66-fresh and UiO-66-UV-vis-5th under dark and light conditions.

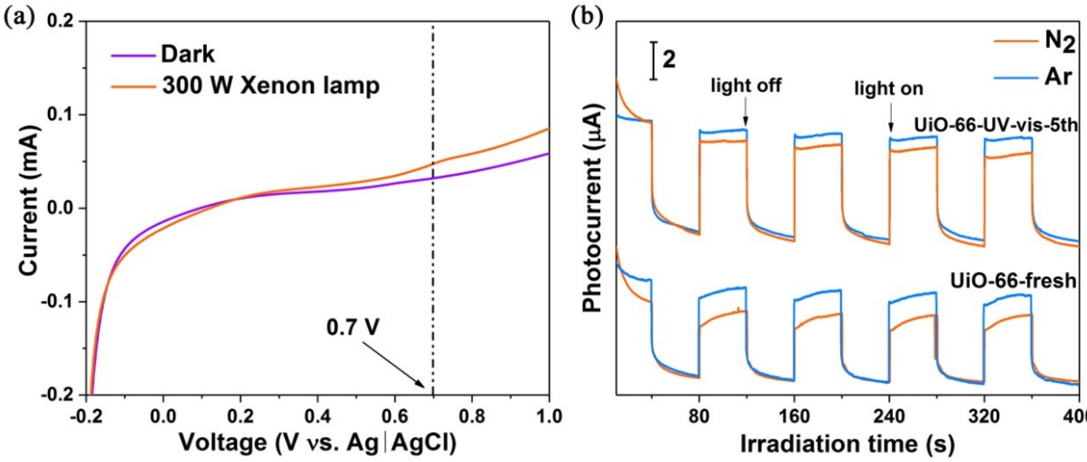

Figure S15. (a) Linear sweep voltammetry (LSV) spectra of the UiO-66 under dark condition and 300 W Xenon light irradiation in N_2 ambient, and (b) Photocurrent spectra of UiO-66-fresh and UiO-66-UV-vis-5th.

Before the photocurrent measurements, the linear sweep voltammetry test was conducted under dark condition and 300 W Xenon light irradiation in N_2 ambient to determine the bias voltage was 0.7 V.

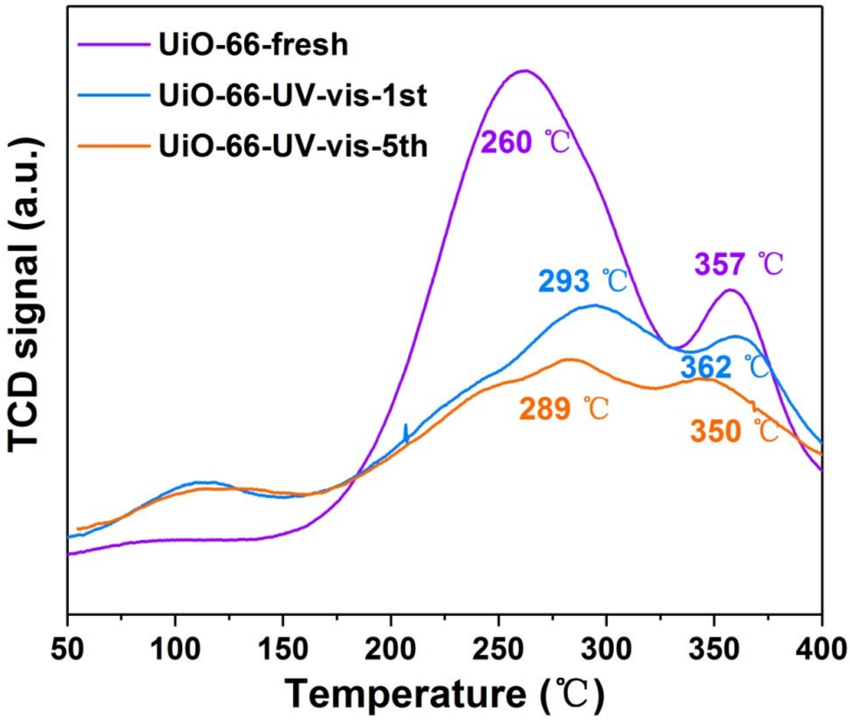

Figure S16. N_2-TPD spectra of UiO-66-fresh, UiO-66-UV-vis-1st, and UiO-66-UV-vis-5th.

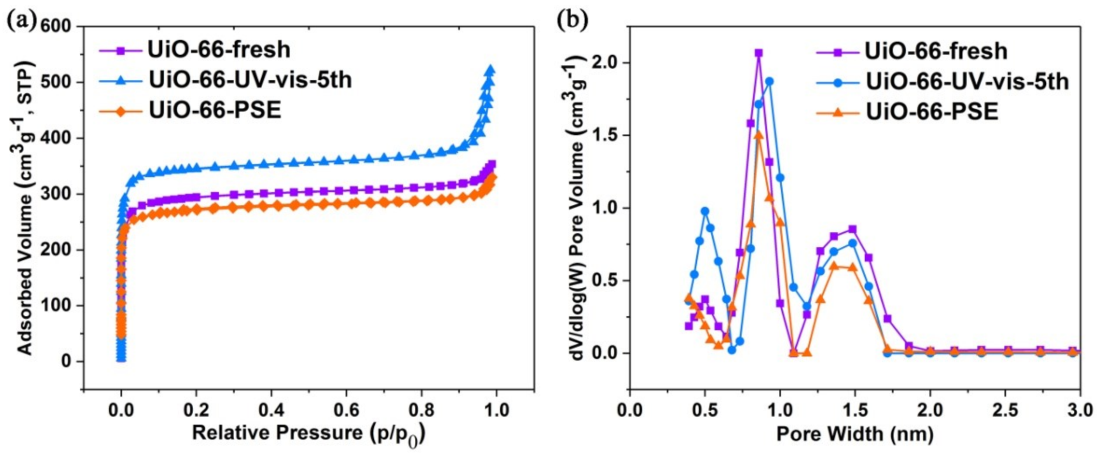

Figure S17. (a) N_2 adsorption-desorption isotherms, and (b) pore size distribution curves of UiO-66-fresh and UiO-66-UV-vis-5th and UiO-66-PSE.

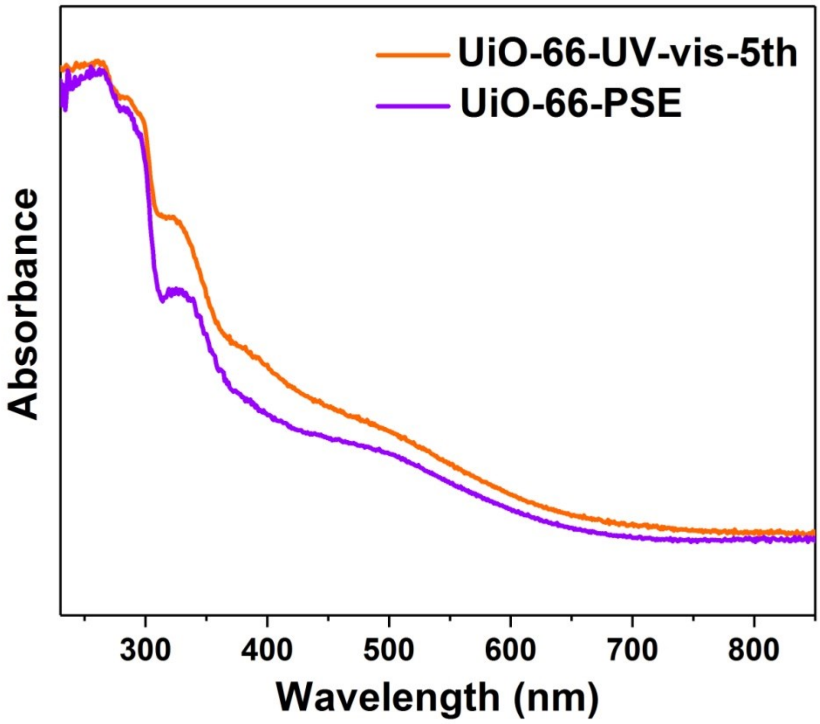

Figure S18. The UV-vis diffuse reflectance spectra (UV-vis DRS) of UiO-66-UV-vis-5th and UiO-66-PSE.

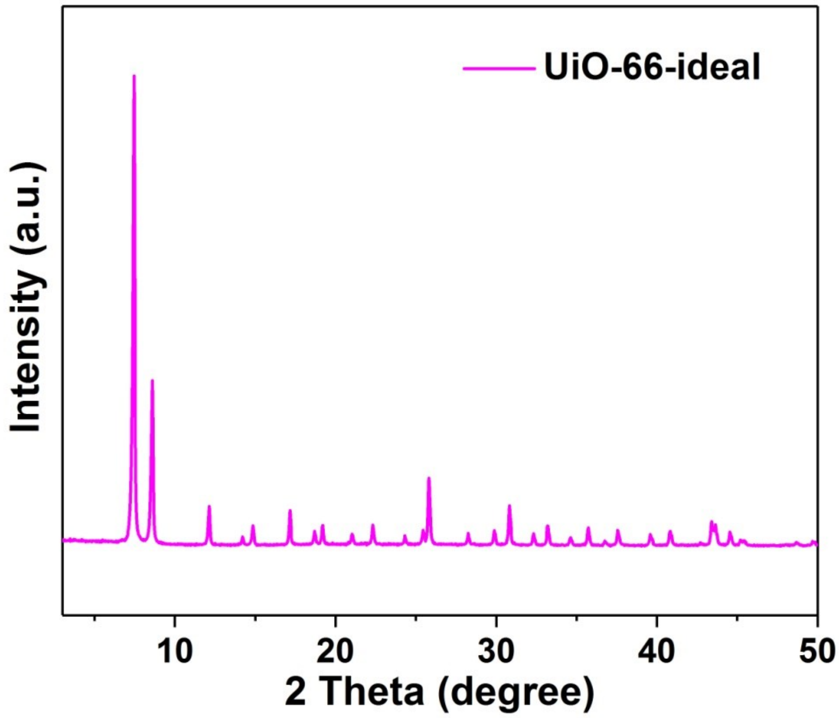

Figure S19. XRD pattern of UiO-66-ideal.

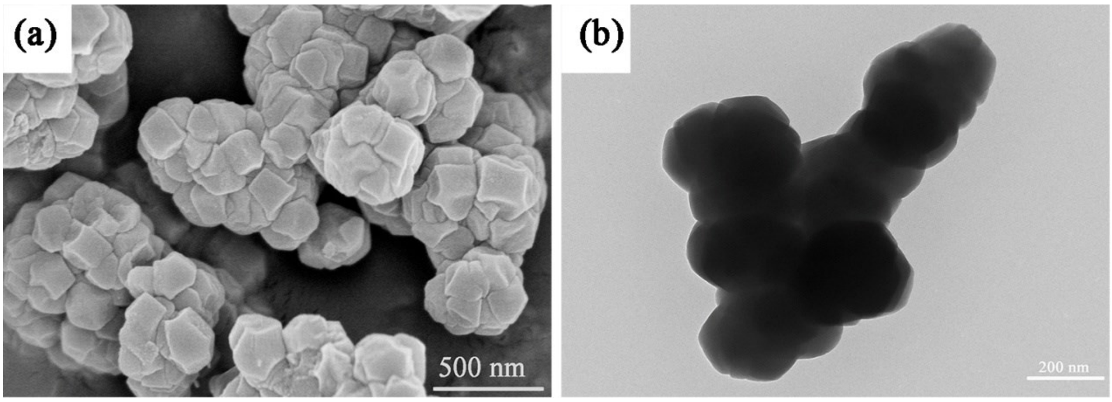

Figure S20. (a) Scanning electron microscopy (SEM) images and (b) Transmission electron microscopy (TEM) images of UiO-66-ideal.

Table S1 Comparison of physical properties of the samples

Photocatalyst	Surface area ($m^2 \cdot g^{-1}$)	Mean pore diameter (nm)	Total pore volume ($cm^3 \cdot g^{-1}$)
UiO-66-fresh	995	2.12	0.416
UiO-66-UV-vis (UiO-66-UV-vis-1st)	1225	2.77	0.519
UiO-66-UV-vis-5th	1144	2.82	0.493
UiO-66-ideal	819	2.10	0.388

Table S2 Comparison of nitrogen photofixation rate with various MOF photocatalysts

Photocatalyst	Reaction medium	Scavenger	Light source	Nitrogen source	NH_3 yield	Reference
UiO-66	**H_2O**	**No**	**UV-vis**	**N_2**	**256 μmol g^{-1} h^{-1}**	**This work**
				Air	**196 μmol g^{-1} h^{-1}**	
			λ≥ 420 nm	**N_2**	**97 μmol g^{-1} h^{-1}**	
				Air	**70 μmol g^{-1} h^{-1}**	
Ti_3C_2-QD/Ni-MOF	H_2O+ $NaSO_3$	1 mM $NaSO_3$	UV-vis	N_2	88.79 μmol g^{-1} h^{-1}	1
MIL-53 (Fe II/Fe III)	H_2O+ K_2SO_3	0.158 g/L K_2SO_3	λ≥ 420 nm	N_2	306 μmol g^{-1} h^{-1}	2
Gd-IHEP-7	H_2O	No	UV-vis	N_2	128 μmol g^{-1} h^{-1}	3
Gd-IHEP-8					220 μmol g^{-1} h^{-1}	
g-C_3N_4/MOF-74 (Zn)	H_2O+ Methanol	Methanol (4% wt)	λ≥ 400 nm	Air	1.7 mmol g^{-1} h^{-1}	4
MIL-101 (Fe)	H_2O	No	UV-vis	N_2	100 μmol g^{-1} h^{-1}	5
NH_2-MIL-125 (Ti)	H_2O	No	λ≥ 400 nm	N_2	12.25 μmol g^{-1} h^{-1}	6
Ce-MOF	H_2O	No	UV-vis	N_2	34 μmol g^{-1} h^{-1}	7

References:

1 J. Z. Qin, B. J. Liu, K.-H. Lam, S. J. Song, X. Y. Li and X. Hu, *ACS Sustain. Chem. Eng.*, 2020, **8**, 17791-17799.

2 Z. F. Zhao, D. Yang, H. J. Ren, K. An, Y. Chen, Z. Y. Zhou, W. J. Wang and Z. Y. Jiang, *Chem. Eng. J.*, 2020, **400**, 125929.

3 K. Q. Hu, P. X. Qiu, L. W. Zeng, S. X. Hu, L. Mei, S. W. An, Z. W. Huang, X. H. Kong, J. H. Lan, J. P. Yu, Z. H. Zhang, Z. F. Xu, J. K. Gibson, Z. F. Chai, Y. F. Bu and W. Q. Shi, *Angew. Chem. Int. Edit.*, 2020, **59**, 20666-20671.

4 Z. Ding, S. Wang, X. Chang, D. H. Wang and T. H. Zhang, *RSC Adv.*, 2020, **10**, 26246-26255.

5 G. Q. Li, F. F. Li, J. X. Liu and C. M. Fan, *J. Solid State Chem.*, 2020, **285**, 121245.

6 H. Huang, X. S. Wang, D. Philo, F. Ichihara, H. Song, Y. X. Li, D. Li, T. Qiu, S. Y. Wang and J. H. Ye, *Appl. Catal. B*, 2020, **267**, 118686.

7 C. Zhang, Y. Xu, C. Lv, X. Zhou, Y. Wang, W. Xing, Q. Meng, Y. Kong and G. Chen, *ACS Appl. Mater. Inter.*, 2019, **11**, 29917-29923.